Preliminary Studies of New Proteasome Inhibitors in the Tumor Targeting Approach: Synthesis and in Vitro Cytotoxicity

Magali Vivier,*,† Anne-Sophie Jarrousse,† Bernadette Bouchon,† Marie-Josephe Galmier,† Philippe Auzeloux,† Jacques Sauzieres,‡ and Jean-Claude Madelmont*,†

UMR 484 INSERM-Université d'Auvergne-Centre Jean Perrin, Rue Montalembert, B.P. 184, 63005 Clermont-Ferrand Cedex, France, and OTL Pharma, 15 Rue de Turbigo, 75002 Paris, France

Received February 25, 2005

The proteasome is a multicatalytic protease that plays a critical role in the cell. The control of proteasomes could, thus, provide a weapon for the treatment of cancer. Therefore, we have synthesized six new peptide aldehyde inhibitors of the proteasome linked to the *N*-(2-diethylaminoethyl)benzamide (BZA-CO) structure, in order to target the cytotoxic activity to malignant melanoma cells. Biological studies demonstrated the influence of length and composition of the amino acid chain on the cytotoxicity of our compounds. Among them, compound **19** presents the highest cytotoxicity ($IC_{50} = 0.64 \pm 0.07$ μmol): this cytotoxicity was maintained in the presence of BZA-CO but decreased 8-fold compared to the control MG132. Fluorescence activated cell sorter (FACS) and cytotoxic activity analysis demonstrated the selectivity of compound **19** for melanoma cells. Finally, western blottings of ubiquitinated proteins in IPC227F cells as well as proteasome assays confirmed that the cytotoxicity was linked to an inhibition of the proteasome activity.

Introduction

The 26S proteasome is a multicatalytic protein complex which is implicated in the degradation of the majority of cellular proteins. It consists of a stack of two α and two β rings. The seven different α-type subunits form the two outer rings of the proteasome 20S cylinder, whereas the seven β-type subunits are components of the two inner rings of the complex. In mammalian cells, this 20S proteolytic component is capped by a regulatory 19S complex at each extremity whose role is to unfold the protein substrates and to stimulate proteolytic activity. This complex exhibits at least five endopeptidase activities. The three principal activities are referred to as chymotrypsin-like (ChT-L) when cleavage occurs on the carboxyl side of hydrophobic residues, trypsin-like (T-L) when cleavage occurs on the carboxyl side of basic amino acids, and post-glutamyl peptide-hydrolyzing (PGPH) when cleavage occurs on the carboxyl side of acidic residues. The two minor peptidase activities cleave peptide bonds after branched-chain (BrAAP) or small neutral amino acids (SNAAP) preferring activity.[1] These proteolytic activities confer on proteasomes more of a recycler function for damaged or misfolded proteins in the cell as well as a critical role in a large panel of events including cell immune surveillance,[2,3] inflammatory response,[4] muscle atrophy,[5] metabolic pathway regulation,[6] circadian rhythm regulation,[7] and transcriptional regulation or cell cycle control.[8,9] The latter is very important, since transcriptional factors modulate cell division and could contribute to tumor growth. These features make proteasomes an interesting new target for anticancer drugs.[10−14] Many natural or synthetic inhibitors of the proteasome have been developed (lactacystin,[15−17] TMC95,[18] peptide aldehydes,[19−22] peptide boronates,[23,24] peptide vinyl sulfones,[25,26] epoxyketones,[27] peptide α-keto aldehydes[28] and α-ketoamides, 5-methoxy-1-indanone-3-acetic peptide derivatives,[29] and bivalent inhibitors[30,31]). All synthetic inhibitors present a peptide structure necessary for the specific recognition by the proteasome site and a cytotoxic moiety such as an aldehyde, boronate, or vinyl sulfone residue. Crystallography and site-directed mutagenesis studies demonstrated that these inhibitors interact with the *N*-terminal threonine (Thr 1) of the three proteolytically active β-subunits.[32−36] Additional residues located close to the active site participate in the catalysis mechanism, but their precise function has not yet been determined. Among the proteasome inhibitors that are under development, the dipeptidyl boronic acid PS-341 (Bortezomib VELCADE, Figure 1)[13,37,38] is commercialized. This compound appears to be particularly interesting for the treatment of several hematologic malignancies (particularly multiple myeloma) and solid tumor indications. Peptide aldehyde inhibitors also represent a very important class among the proteasome inhibitors. According to Kisselev et al.,[11] these inhibitors are an essential family for studies in cell culture and tissues. Indeed, MG132 (Figure 1) was one of the first synthetic inhibitors to be described and used in the inhibition of proteasomes. As a peptide aldehyde inhibitor, MG132 has the advantage of dissociating from the proteasome, conferring rapid reversibility of its action. Moreover, MG132 has mainly been studied for its significant cytotoxic activity.[39] Nevertheless, the ubiquitous properties of the proteasome limit the use of the proteasome inhibitors in any therapy. The alternative

* Authors for correspondence. Phone: (33) 4 73 15 08 00. Fax: (33) 4 73 15 08 01. E-mail: vivier@inserm484.u-clermont1.fr or madelmont@inserm484.u-clermont1.fr.
† UMR 484 INSERM-Université d'Auvergne-Centre Jean Perrin
‡ OTL Pharma.

10.1021/jm050181l CCC: $30.25
Published on Web 09/27/2005

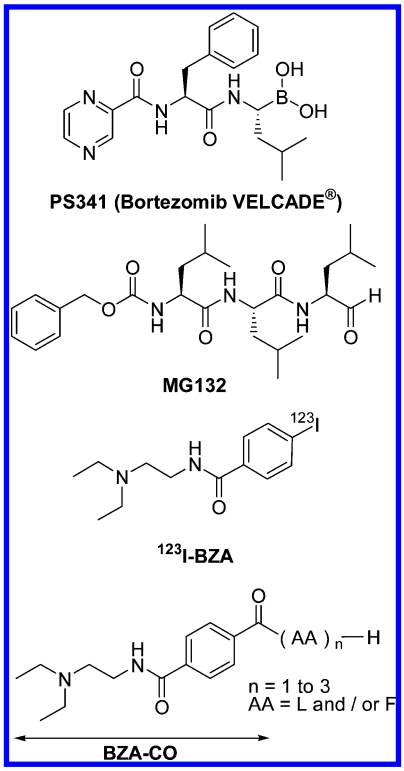

Figure 1. Pharmacomodulated proteasome inhibitors: a coupling between ^{123}I-BZA and proteasome inhibitors.

way to overcome this limit would be to carry these drugs selectively to the target tumoral tissue.

On this basis, our laboratory has had great experience in targeting melanoma cells: Moreau et al.[40] have developed in our laboratory a new radiopharmaceutic [^{123}I]-*N*-(2-diethylaminoethyl)-4-iodobenzamide (^{123}I-BZA, Figure 1) which binds to melanin pigmented cells with high affinity. This radiopharmaceutic has been used in previous scintigraphic studies in humans and presents a sensitivity of over 80% and a specificity of 100% localization on malignant melanomas and metastases.[40−47]

Therefore, along with other studies we initiated on potent and selective cytotoxic antitumor agents, we decided to synthesize new peptide aldehyde inhibitors of the proteasome linked to the *N*-(2-diethylaminoethyl)-benzamide structure (BZA-CO, Figure 1) in order to target the cytotoxic activity to malignant melanoma cells.

This is the first report of the synthesis and pharmacological characterization of six peptide aldehydes linked to the benzamide derivative structure (Figure 2). The effects of the introduction of BZA-CO into the peptide aldehyde structure on the cytotoxicity, length, and composition of the amino acid chain are also discussed. The measurement of the three main proteasome activities is also reported.

Results and Discussion

Synthesis of Peptide Inhibitors. Two methods were investigated to synthesize the vector structure precursor **7** (Scheme 1). First, we used the iodine and bromine precursors **1** and **2** which were directly transformed into the carboxylic acid derivative **4** by CO_2 carbonation[48] through the lithium reagent.[49] As these reactions gave insufficient yields (21% and 9%, respectively), probably due to the poor formation of the lithium derivative, we favored route b, reaction of 2-diethylaminoethylamine with dimethylterephthalate in the presence of trimethylaluminum. The monosubstituted derivative **5** (70% from **3**) and the disubstituted derivative **6** (2% from **3**) obtained by this route can be easily separated by flash chromatography. The ester **5** was transformed into the lithium salt **7** by saponification at room temperature with lithium hydroxide (method B in the Experimental Section) in quantitative yield.[50]

General synthetic pathways to obtain peptide structures are presented in Scheme 2. The final leucine derivatives **13**, **16**, and **19** were prepared by following two different routes. Whenever possible, commercially available protected amino acids were employed. In the first step, leucine-derivative-structured peptides **11**, **14**, and **17** (route A) were prepared using standard peptide synthesis procedures, with DCC and HOBt as catalytic coupling agents.[51−59] Protecting groups were removed by treatment with lithium hydroxide for the methyl group or with trifluoroacetic acid (TFA) for the *tert*-butyl carbamate (Boc) group. In the next step, the coupling reactions between the acid **7** and amines **8**, **11**, **14**, and **17** were undertaken in the presence of coupling reagents DCC or HOBt according to method C. An example of synthetic routes A and B is provided by the preparation of compound **12**. According to route A, methyl leucine ester hydrochloride **8** was coupled to compound **7** to give compound **9** with acceptable yield (51%, method C in the Experimental Section). The methyl-protective group of compound **9** was removed by saponification with lithium hydroxide (method B)[50] to give compound **10** in good yield (89%). However, the coupling reaction between **10** and *N,O*-dimethylhydroxylamine hydrochloride (method C) gives compound **12** in very weak yield. This may be due to the steric hindrance of the *N*-(diethylaminoethyl) chain. Consequently, we decided to investigate route B. Using this route, the coupling reaction between acid **7** and compound **11** allowed us to prepare compound **12** with sufficient yield (12%). The Weinreb amide thus obtained was reduced with $LiAlH_4$ (method D in the Experimental Section) to give corresponding aldehyde **13** with quantitative yield.[39]

In summary, since route B gave better yield for the synthesis of **13**, **16**, and **19**, we used this synthetic route to prepare compounds **22**, **25**, and **28** (Scheme 3). The pure peptide aldehyde products **13**, **16**, **19**, **22**, **25**, and **28** were isolated as white solids by recrystallization from diethyl ether and were tested as hydrochloride salts.

Biological Studies. Attached human ocular melanoma IPC227F cells were cultured for 24 h on a microplate and then exposed for 48 h to increasing concentrations of the peptide aldehydes **13**, **16**, **19**, **22**, **25**, and **28** or MG132 as a control. The effect of these compounds on cell outgrowth was evaluated by assay with Hoechst dye 33342. First, we wanted to demonstrate that the link from peptide aldehydes to a melanoma vector preserved a cytotoxicity. We also investigated the effects on cytotoxicity of the substitution of the Cbz protected group in MG132 by BZA-CO (compound **19**). As shown in Figure 3A, the cytotoxicity of compound **19** was maintained ($IC_{50} = 0.64 \pm 0.07$ μM) but has decreased 8-fold compared to that of the MG132 control ($IC_{50} = 0.077 \pm 0.009$ μM). The influence of

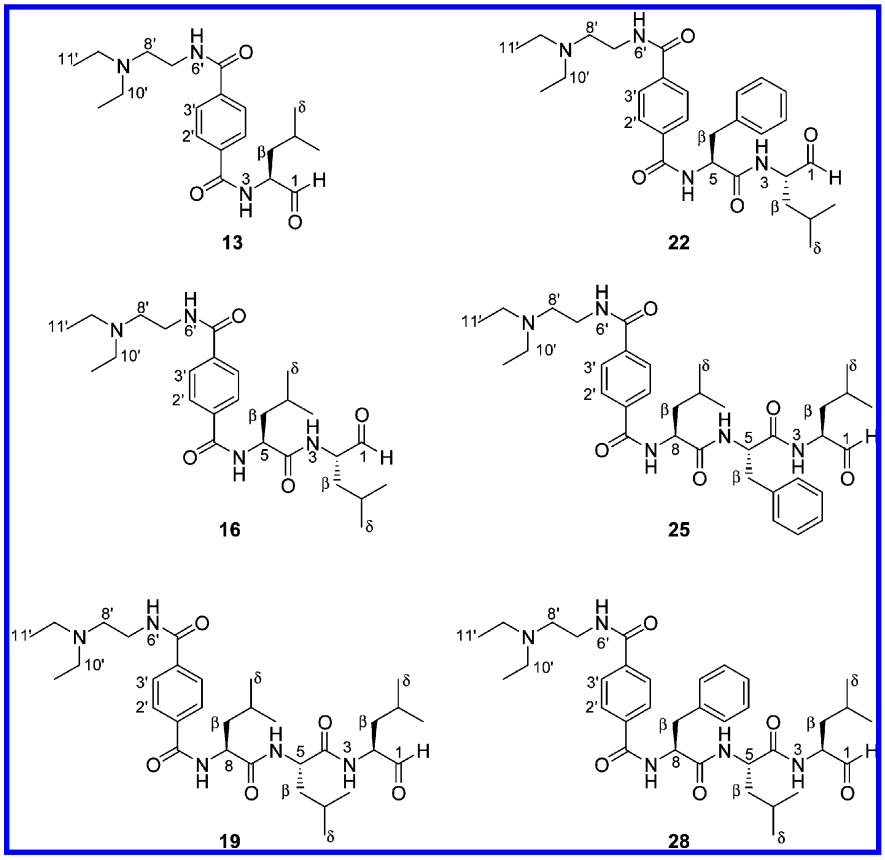

Figure 2. Synthesized peptide aldehydes.

Scheme 1. Synthesis of BZA-CO Precursor[a]

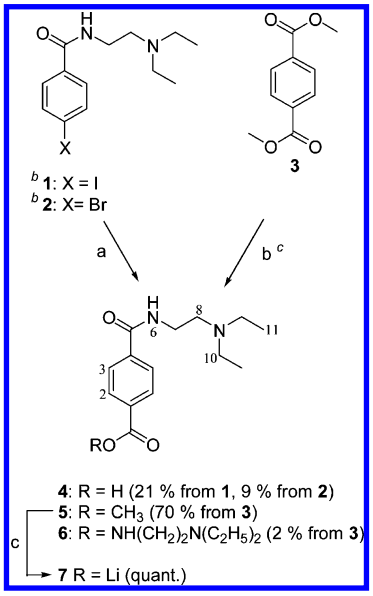

[a] Reagents: (a) BuLi, CO_2, Et_2O or Et_2O/THF, −70 °C; (b) $NH_2CH_2CH_2NEt_2$, $Al(CH_3)_3$, CH_2Cl_2, reflux; (c) LiOH, THF/H_2O, room temperature (rt). [b] Compounds **1** and **2** are synthesized as already published.[45] [c] Route b is preferred to route a.

Scheme 2. General Methods for the Preparation of Leucinal Derivates[a]

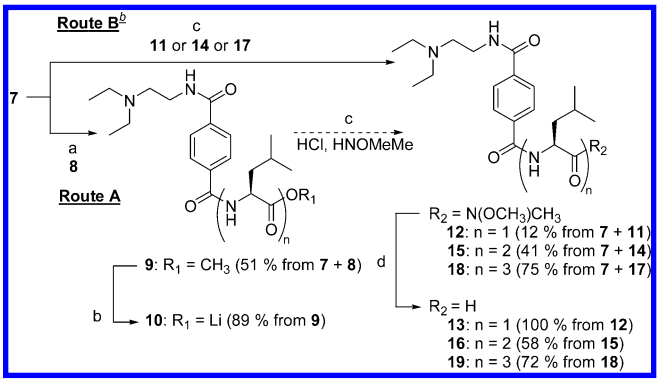

[a] Reagents: (**8**) HCl, Leu-OMe; (**11**) TFA-Leu-NOMeMe; (**14**) TFA-Leu-Leu-NOMeMe; (**17**) TFA-Leu-Leu-Leu-NOMeMe. (a) DCC, HOBt, TEA, CH_2Cl_2 or CH_2Cl_2/DMF, rt; (b) LiOH, THF/H_2O, rt; (c) DCC, HOBt, TEA, CH_2Cl_2 or CH_2Cl_2/DMF or BOP, DMF, TEA, rt; (d) $AlLiH_4$, THF, −80 °C. [b] Route B is preferred to route A.

pharmacomodulation on the cytotoxicity of the peptide chain was then estimated. According to different previous optimization studies,[23,25,27−29] all the peptide aldehydes synthesized here contained a leucine at the P_1 position: this leucine should increase the chymotrypsin-like activity of these inhibitors.[27] Comparisons were made of the cytotoxicity of compounds **13**, **16**, and **19** that contained one, two, or three leucine residues, respectively. As shown in Figure 3A, in contrast to compound **19**, the compounds with one or two leucine residues (**13** and **16**) were inefficient at inhibiting cell growth. Thus, it appears that the length of the amino acid chain could play a major role in cytotoxic activity. These results corroborate those previously obtained with epoxide proteasome inhibitors.[27]

Since the dipeptidyl inhibitor PS-341 contains leucine and phenylalanine residues,[23] the effect of amino acid chain composition on cytotoxicity was investigated. The comparison of cytotoxicities between compounds **16** and **22** that contained two leucine residues or a leucine and a phenylalanine residue, respectively. Figure 3B and Table 1 showed that the presence of phenylalanine at the P_2 position dramatically enhanced potency (IC_{50} =

Scheme 3. Synthesis of Compounds **22**, **25**, and **28**[a]

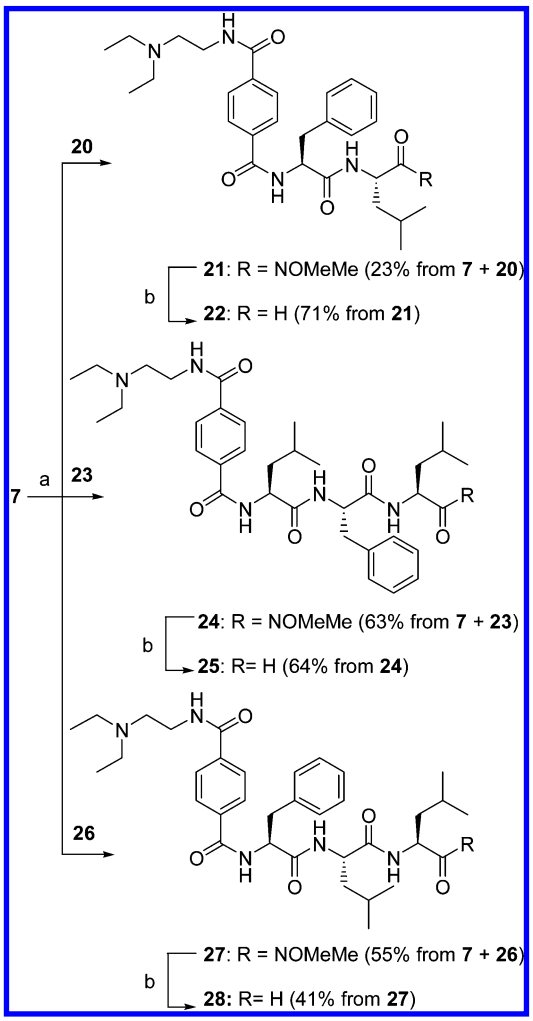

[a] Reagents: (**20**) TFA-Phe-Leu-NOMeMe; (**23**) TFA-Leu-Phe-Leu-NOMeMe; (**26**) TFA-Phe-Leu-Leu-NOMeMe. (a) DCC, HOBt, TEA, CH_2Cl_2 or CH_2Cl_2/DMF, rt; (b) $AlLiH_4$, THF, −80 °C.

20.88 ± 1.96 μM for compound **22** versus no inhibition observed for compound **16**).

Conversely, the comparison of the tripeptidyl compounds **19**, **25**, and **28** that contained, respectively, three leucine residues, a phenylalanine at the P_2 position, and a phenylalanine at the P_3 position showed that the presence of a phenylalanine did not increase cytotoxicity (Figure 3C and Table 1). Indeed, the IC_{50} values of **25** and **28** were, respectively, 4.5-fold and 18-fold higher than that of **19**. However, the migration of the phenylalanine from the P_2 to the P_3 position (compounds **25** and **28**) increased cytotoxicity by 4-fold. These results are in accordance with the study on epoxycetones already published by Eloffson et al.[27] In summary, at equal chain lengths, amino acid composition plays a key role in obtaining sufficient toxicity.

We attempted then to correlate the cytotoxic activity to the proteasome inhibition. To confirm that these newly synthesized molecules inhibited proteasome, we observed the accumulation of ubiquitinated proteins in IPC227F cells. The proteins were tagged with several ubiquitin molecules in order to be recognized and degraded by the proteasomes. Therefore, the inhibition of the proteasome was able to lead to the accumulation of ubiquitinated proteins (Figure 4).[8,9,21,38,60,61] IPC227F cells were then treated at various time intervals with

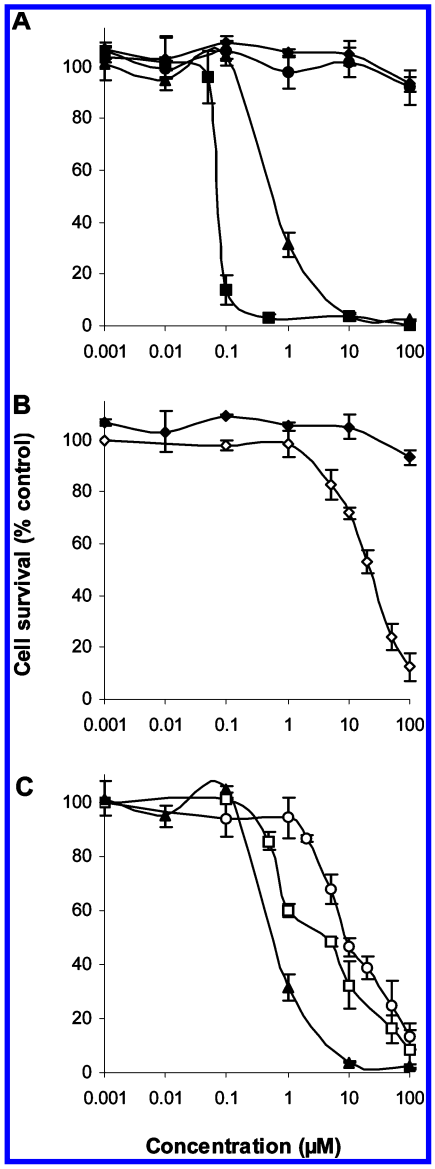

Figure 3. Cytotoxicity assay. Attached IPC227F cells were incubated with increasing concentrations of (A) MG132 (■), **13** (●), **16** (◆), or **19** (▲); (B) **16** (◆) or **22** (◇); or (C) **19** (▲), **25** (○), or **28** (□) for 48 h, washed with 1X PBS, and then frozen at −80 °C. Cell survival data were determined using fluorescent Hoechst dye 33342. The data are expressed as mean percentages ± standard deviation (SD) of the untreated control (n = 3).

10 μM cytotoxic drugs **19**, **22**, **25**, and **28**, and following extraction, the accumulation of polyubiquitinated proteins was visualized as a dark smear of proteins by Western blotting using anti-ubiquitin antibody. As shown in Figure 5, under the conditions used, only compound **22** did not lead to the accumulation of ubiquitinated proteins, even after 48 h of incubation. This could indicate that the cytotoxic effect of compound **22** leads to some result other than proteasome inhibition. However, incubation of IPC227F cells with **19**, **25**, or **28** produced an accumulation of ubiquitin-tagged proteins in a time-dependent manner, since a smear appeared after 24 h of incubation. These observations are perfectly comparable to those obtained with the reference product MG132.

Finally, to confirm that the accumulation of ubiquitin-tagged proteins observed is due to proteasome inhibi-

Table 1. Concentration Inhibiting 50% of Cell Growth (IC_{50}) in IPC227F Cells[a]

G——P_3——P_2——P_1——CHO

cpd	G[b]	P_3	P_2	P_1	IC_{50} (μM)
MG132	Cbz	leu	leu	leu	0.077 ± 0.009
13	BZA-CO			leu	NI[c]
16	BZA-CO		leu	leu	NI[c]
19	BZA-CO	leu	leu	leu	0.64 ± 0.07
22	BZA-CO		phe	leu	20.88 ± 1.96
25	BZA-CO	leu	phe	leu	2.84 ± 0.34
28	BZA-CO	phe	leu	leu	11.92 ± 1.20

[a] IC_{50} values are determined from the survival curves. Values are the means ± SD from three independent experiments, each of which was performed in triplicate. All the compounds are tested as chlorhydrate salts. [b] Cbz = Ph−CH_2−O−CO−; BZA = Et_2−NH−$(CH_2)_2$−NH−CO−C_6H_4−. [c] No inhibition observed.

tion, the three main proteasome activities, i.e., ChT-L, T-L, and PGPH activities, were measured on 20S proteasomes incubated with compounds **19**, **25**, and **28**. As shown in Figure 6A, the three compounds tested reduced the ChT-L activity (70−95% inhibition) in a dose-dependent manner (0.1−10 μM), whereas we did not observe any significant decrease of the T-L activity (Figure 6B). These results are in agreement with results published by Eloffson et al.[27] and Stein et al.[39] We wanted to increase the ChT-L activity of pharmacomodulated inhibitors by the introduction of leucine at the P_1 position. Concerning the PGPH activity (Figure 6C), only compounds **19** and **25** were efficient in a dose-dependent manner, similar to the MG132 control. However, these percentages of inhibition measured for PGPH activity were less important than the one observed for the ChT-L activity (approximately 40−80%). Compound **28** appeared to be less effective with a global inhibition rate of 35%. These results confirmed that the cytotoxic activity toward melanoma cells and the accumulation of ubiquitinated proteins after treatment with compounds **19**, **25**, and **28** are indeed correlated to the inhibition of proteasomes by these new molecules.

At last, we observed that compound **19** exhibited a high cytotoxic activity in IPC227 F cells (IC_{50} = 0.64 ± 0.07μM) but failed to exhibit a cytotoxic activity in normal melanocytes, with IC_{50} values higher than 100 μM (Figure 7). These preliminary results are consistent with the selectivity of the compounds for melanoma cells. Furthermore, FACS analysis did not demonstrate any changes in percentages in the different phases of the cell cycle in the normal melanocytes treated by compound **19** (Figure 8A). Conversely, the percentages in the M_4Beu cells (human melanoma cells) treated by compound **19** increased in phase G_2M and decreased in phase S (Figure 8B). These results of the cell cycle profile confirm the hypothesis of selectivity of our compounds in favor of melanoma cells.

Conclusion

In this study, we report the synthesis and pharmacological characterization of six leucine peptides linked to the benzamide structure. It appears that the introduction of the BZA-CO cluster to the peptidyl Weinreb amide (route B) gives a better yield than the formation of the Weinreb amide at the last step (route A). Biological studies demonstrated that the compounds with one or two leucine residues (**13** and **16**) were inefficient at inhibiting cell growth. The presence of the phenylalanine at the P_2 position appeared to increase the cytotoxicity of the dipeptidyl aldehydes (compound **22**) but, surprisingly, did not increase the cytotoxicity of the tripeptidyl aldehydes (compounds **25** and **28** versus **19**). In summary, among all the compounds tested, the derivative **19** presented the highest cytotoxicity (IC_{50} = 0.64 ± 0.07 μmol): although cytotoxicity decreased 8-fold in comparison to that of the control MG132, the substitution of the Cbz protective group by the BZA-CO cluster maintained a significant cytotoxicity on human ocular melanoma IPC227F cells.

The accumulation of polyubiquitinated proteins in IPC227F cells and proteasomes assays confirmed that the cytotoxicity observed after incubation in the presence of pharmacomodulated compounds was due to proteasome activity inhibition.

The preliminary results concerning the selectivity of our compounds for melanoma cells have demonstrated their low cytotoxicity in normal melanocytes. The drug biodistribution of the ^{125}[I] derivative of compound **19** was also studied in mice bearing subcutaneous implantation of malignant melanoma cells. These experiments showed an accumulation of 2.7% injected dose per gram (DI/g) of this compound in B16 tumors at 15 min, with 1.2% of this aldehyde remaining in the tumor at 3 and 6 h after administration, thus giving a tumor/muscle ratio of over 2.3 (data not shown). These two results are in accordance with the selectivity for melanoma cells of our pharmacomodulated derivatives.

This compound conjugation approach will be entirely validated after in vivo experiments on tumor-bearing animals with radiolabeled compounds in order to verify the selectivity of the compounds to malignant melanomas and metastases.

Experimental Section

Chemistry. All reagents and solvents were from commercial suppliers and used with no further purification. Tetrahydrofuran (THF) was distilled over sodium-benzophenone. All other reaction solvents were anhydrous or high-performance liquid chromatography (HPLC) commercial grades (Carlo Erba Reagenti, Milan, Italy). Compound purity was checked by thin layer chromatography (TLC) on precoated silica gel plates (plastic sheet 60 F_{254}, layer thickness 0.25 mm; SDS, Pepin, France), aluminum oxide plates (60 F_{254}, neutral type E, layer thickness 0.20 nm; Merck, Darmstadt, Germany), or RP-18 plates (RP-18 F_{254S}; Merck) using DCM/MeOH 98/2% (solvent mixture A) or H_2O/CH_3CN/TFA 40/60/0.1% (solvent mixture B). Melting points were determined with a Reichert−Jung−Koffler apparatus. Infrared spectra were recorded in KBr pellets or in CCl_4 on an FT Vector 22 instrument (ν expressed in cm^{-1}; Bruker, Bremen, Germany, developed in the Supporting Information). Proton and carbon magnetic resonance spectra (^{1}H and ^{13}C NMR) were performed in $CDCl_3$ or DMSO-d_6 on a Bruker AM 200 (4.7 T) or a Bruker DRX 500 (11.7 T) spectrometer (developed in the Supporting Information). Chemical shifts (δ) are reported in parts per million relative to the internal standard $(CH_3)_3Si$ or relative to solvent signals ($CDCl_3$, δ = 7.26 ppm for ^{1}H NMR and δ = 77.0 ppm for ^{13}C NMR, or DMSO-d_6, δ = 2.49 ppm for ^{1}H NMR and δ = 39.0 ppm for ^{13}C NMR). Electrospray ionization mass spectra (ESI-MS) were obtained on a ESQUIRE-LC spectrometer in positive or negative mode (solvent: CH_3CN or CH_3CN/H_2O 1:1; Bruker). Main fragmentations of $[M + H]^+$ ions derived from the electrospray of synthesized derivatives have been determined (developed in the Supporting Information). The amino acids required for the preparation of inhibitors **11**,

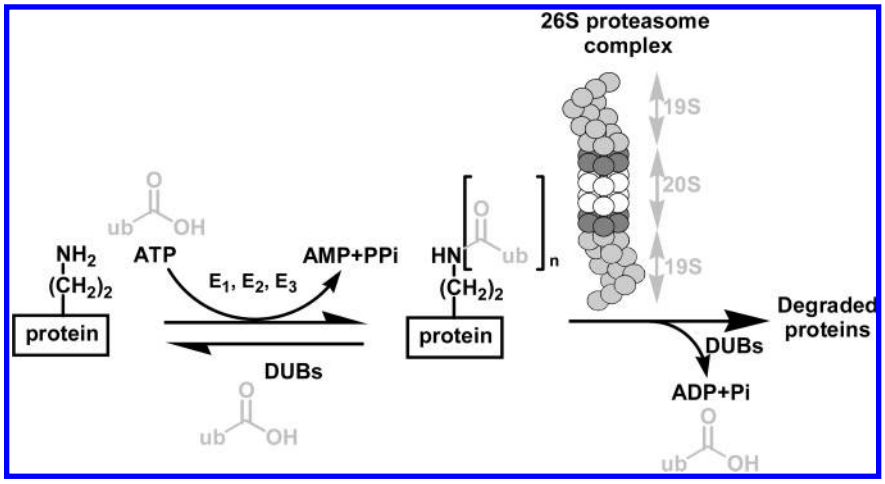

Figure 4. Ubiquitin−proteasome protein degradation. The process starts with the ATP-dependent activation of ubiquitin (Ub-COOH) by an ubiquitin-activating enzyme (E_1), followed by transfer to an ubiquitin-conjugating enzyme (E_2) and, finally, attachment of the ubiquitin to the protein substrate with or without the help of the ubiquitin−protein ligases (E_3). The polyubiquitinated substrate is recognized and subsequently degraded by the 26S proteasome. The ubiquitin monomers are reclaimed by the action of deubiquinylating enzymes (DUBs). These last enzymes are responsible for the recycling of the ubiquitin back into the pool of free ubiquitin in the cell.

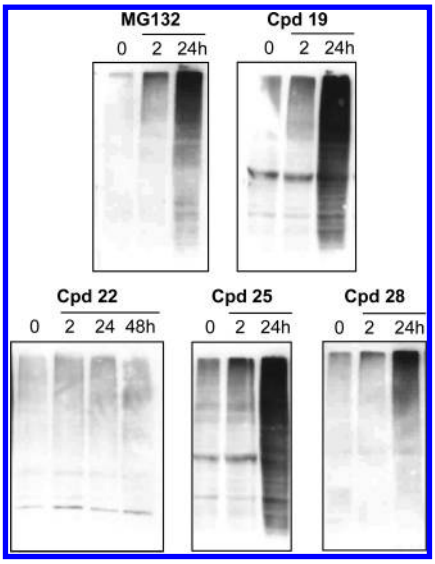

Figure 5. Accumulation of polyubiquitinated proteins in IPC227F cells. IPC227F cells were treated for different time intervals with 10 μM MG132 or compound (Cpd) **19**, **22**, **25**, or **28**. Accumulation of ubiquitin-tagged proteins was evaluated by Western blotting.

14, **17**, **20**, **23**, and **26** were synthesized by standard peptide chemistry methods and/or literature synthesis.

General Method A: 4-(((Diethylamino)ethyl)carbamoylbenzoic Acid (4). To a solution of **1** (2.01 g, 5.81 mmol) in a THF/Et_2O mixture (5 mL/200 mL) at −70 °C was added a solution of *n*-butyllithium 2.5 M/THF (7 mL, 17.5 mmol, 3 equiv) under nitrogen atmosphere. In another ball of the vacuum system, a solution of H_2SO_4 (50 mL) was added to barium carbonate (1.27 g, 6.39 mmol, 1.1 equiv). CO_2 gas formed and was transferred on the reaction mixture at 20 Pa. The mixture was allowed to reach room temperature and then was stirred overnight. The reaction was quenched by water. The aqueous layer (pH = 2) was washed with $CHCl_3$ (3 mL × 50 mL) and then concentrated under reduced pressure to afford 0.3 g of **4** in the form of a hydrochloride salt (yield: 21%): beige solid; mp 186−188 °C; TLC R_f 0.7 (RP-18, solvent mixture B).

Methyl 4-(((Diethylamino)ethyl)carbamoyl)benzoate (5). To a solution of 2-diethylaminoethylamine (10.56 g, 91.0 mmol) in 60 mL of CH_2Cl_2 was added dropwise a solution of trimethylaluminum 2 M in hexane (50 mL, 100 mmol) at 0 °C under a nitrogen atmosphere. The reaction mixture was stirred at 0−5 °C for 2 h and was transferred to a solution of dimethylterephthalate (53.02 g, 273 mmol) in 600 mL of dichloromethane. The reaction mixture was refluxed for 77 h, and then, the reaction was quenched with water (40 mL). The white precipitate obtained was filtrated and extracted with CH_2Cl_2 (4 mL × 100 mL). The combined organic layers were washed with brine, dried over $MgSO_4$, and concentrated in part under vacuum. After addition of methanol, the precipitate of excess of dimethylterephthalate was eliminated by filtration. The filtrate was evaporated under vacuum. Purification was achieved by flash chromatography (aluminum oxide, CH_2Cl_2/MeOH 99.5/0.5) to afford 17.7 g of **5** (yield: 70%) and 0.69 g of **6** (yield: 2%). **5**: white solid; mp 62−64 °C; TLC R_f 0.4 (aluminum oxide, CH_2Cl_2/MeOH 98/2); Anal. ($C_{15}H_{22}N_2O_3$, 0.3 H_2O) C, H, N. **6**: white solid; mp 138−140 °C; TLC R_f 0.2 (aluminum oxide, solvent mixture A).

General Method B. Lithium 4-(((Diethylamino)ethyl)-carbamoyl)benzoate (7). To a solution of lithium hydroxide monohydrate (3.91 g, 93.3 mmol, 1.5 equiv) in water (100 mL) was added dropwise a solution of compound **5** (17.3 g, 62.2 mmol) in THF (150 mL) at 0 °C. The mixture was allowed to reach room temperature and then stirred for 1 h. The reaction mixture was evaporated under reduced pressure, and the crude product was washed with acetone and diethyl ether to afford 16.8 g of **7** (yield: 100%): white solid; mp > 200 °C; TLC R_f 0.7 (RP-18, solvent mixture B); Anal. ($C_{14}H_{19}LiN_2O_3$, 0.75 H_2O, 1.0 LiOH) C, H, N.

General Method C: Methyl 2-(4-(((Diethylamino)ethyl)carbamoyl)benzamido)-4-methylpentanoate (9). To a solution of acid salt **7** (1.80 g, 6.69 mmol) in CH_2Cl_2 at 0 °C were added successively hydroxybenzotriazole (HOBt, 0.16 g, 1.16 mmol, 0.3 equiv), dicyclocarbodiimide (DCC, 1.24 g, 5.99 mmol, 1.15 equiv) and triethylamine (1.60 mL, 16.7 mmol, 2.5 equiv). The mixture was stirred at 0 °C for 1 h. A solution of amine **8** (1.04 g, 5.76 mmol, 1 equiv) in CH_2Cl_2 was added dropwise at 0 °C, and the reaction mixture was then stirred overnight at room temperature. A white precipitate of dicyclohexylurea (DCU) was eliminated by filtration, and the filtrate was washed with a saturated sodium bicarbonate aqueous solution (100 mL) and brine (100 mL), dried over $MgSO_4$, and concentrated under vacuum. The pure compound (**9**) was obtained by recrystallization in diethyl ether (yield: 51%): white solid; mp 162−164 °C.

Lithium 2-(4-(((Diethylamino)ethyl)carbamoyl)benzamido)-4-methylpentanoate (10). Compound **10** was prepared according to method B. Compound **9** (1.63 g, 4.18 mmol) gives after purification 1.2 g of compound **10** (yield: 89%): white solid; mp 179−181 °C; TLC R_f 0.7 (RP-18, solvent mixture B); Anal. ($C_{20}H_{30}LiN_3O_4$, 1.5 H_2O, 0.5 LiOH) C, H, N.

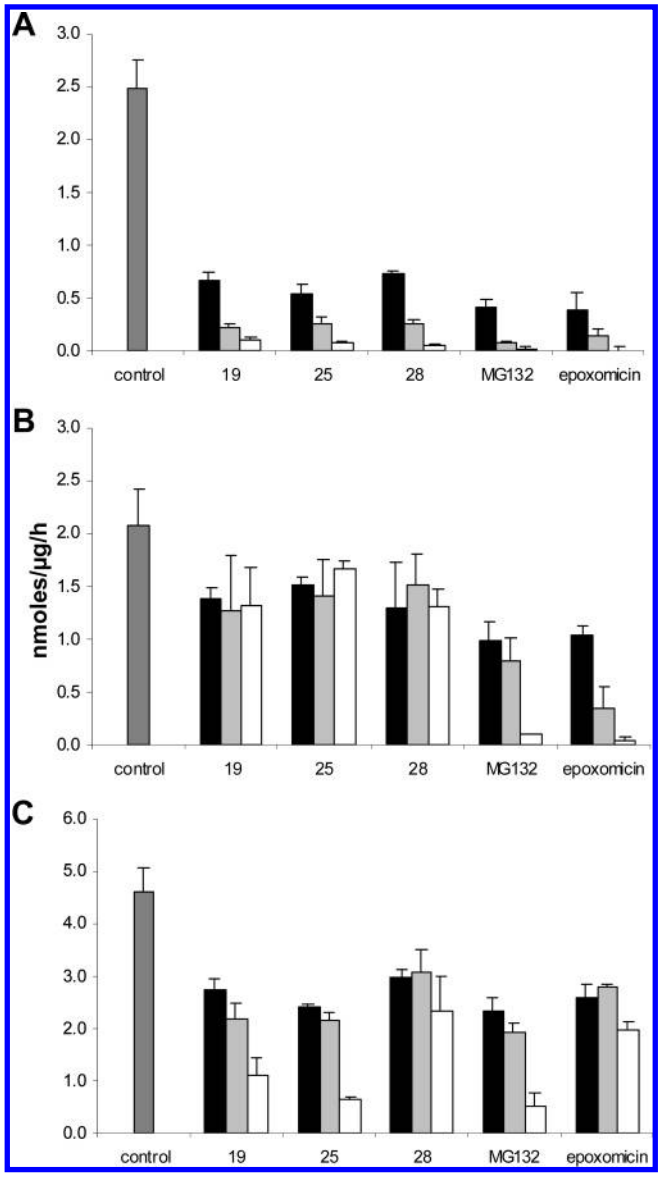

Figure 6. Proteasome inhibition assays. Proteasomes were incubated for 30 min at room temperature in the absence (control, dark gray bars) or presence of 0.1 μM (black bars), 1 μM (light gray bars), and 10 μM (white bars) **19**, **25**, **28**, MG132, or epoxomicin. Assays were then incubated 1 more hour at 37 °C with (A) 100 μM Suc-LLVY-AMC (ChT-L activity), (B) 100 μM Boc-LRR-AMC (T-L activity), or (C) 200 μM Z-LLE-AMC (PGPH activity). Peptidic activities were determined by measuring the liberated fluorophore AMC using a fluorescence microplate reader at 360/460 nm. Values are means ± SD (n = 3).

***N*^{1}-((Diethylamino)ethyl)-*N*^{4}-(1-(methoxy(methyl)amino)-4-methyl-1-oxopentan-2-yl)terephthalamide (12).** The synthesis of **12** was realized according to method C from compound **7** (1.0 g, 3.7 mmol) and compound **11** (1.1 g, 3.7 mmol). The crude product (2.4 g) was purified by flash chromatography (aluminum oxide, CH_2Cl_2/gradient of MeOH 0.5 up to 2%) to afford 0.45 g of **12** (yield: 12%): white solid; mp 120−122 °C; TLC R_f 0.3 (aluminum oxide, solvent mixture A); Anal. ($C_{22}H_{36}N_4O_4$, 1.2 H_2O) C, H, N.

General Method D: Synthesis of *N*^{1}-((Diethylamino)-ethyl)-*N*^{4}-(4-methyl-1-oxopentan-2-yl)terephthalamide (13). A solution of lithium aluminum hydride in ether (0.8 mL, 0.8 mmol, 3 equiv) was added dropwise at −80 °C under a nitrogen atmosphere to a solution of compound **12** (101 mg, 0.24 mmol) in anhydrous THF (4 mL). The mixture was stirred for 90 min and then was allowed to warm to 0 °C. The reaction was quenched by the addition of water (20 mL), and excess lithium aluminum hydride was eliminated by the Mihailovic method. The resulting crude reaction mixture was extracted with CH_2Cl_2 (3 mL × 20 mL). The combined organic layers were washed with brine (10 mL), dried over $MgSO_4$, and concentrated under vacuum to afford 87 mg of compound **13** (yield: 100%). The corresponding hydrochloride was obtained by stirring **13** in ether/HCl 2 N as a very hygroscopic salt. (**13**, HCl): white solid; mp 112−114 °C; TLC R_f 0.4 (aluminum oxide, CH_2Cl_2/MeOH 95/5).

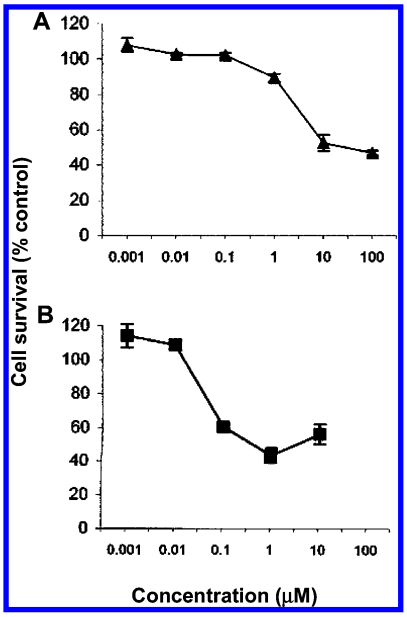

Figure 7. Cytotoxicity assay in normal melanocytes. Normal melanocytes cells (MshL1) were incubated with increasing concentrations of (A) compound **19** or (B) MG132 for 48 h, washed with 1X PBS, and then frozen at −80 °C. Cell survival data were determined using fluorescent Hoechst dye 33342. The data are expressed as mean percentages ± SD of the untreated control (n = 3).

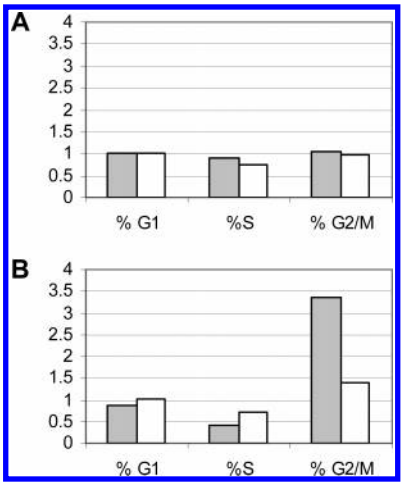

Figure 8. Flow cytometric analysis of human melanoma cells and normal melanocytes. Distribution in a cell cycle of (A) normal melanocytes (MshL1) or (B) M4Beu cells (human melanoma cells) incubated with 10 mM compound **19** or MG132 for 24 h was performed using an Epics XL (Coulter, Hialeah, FL) after propidium iodide labeling of cells and normalized by the ratio of compound **19**/control (light gray bars) or MG132/control (white bars).

***N*^{1}-((Diethylamino)ethyl)-*N*^{4}-(1-(1-(methoxy(methyl)-amino)-4-methyl-1-oxopentan-2-ylamino)-4-methyl-1-oxopentane-2-yl)terephthalamide (15).** To a solution of compound **7** (0.77 g, 2.84 mmol) in DMF (10 mL) were added benzotriazoyloxytris[diethylamino]phosphonium hexafluorophosphate (BOP) (1.38 g, 3.12 mmol) and triethylamine (0.4

mL). The mixture was stirred at room temperature for 15 min, and then, a solution of **14** (1.13 g, 2.83 mmol) in DMF (10 mL) was added. The mixture reaction was stirred overnight at room temperature and evaporated under vacuum. The resulting crude reaction (1.12 g) was purified by flash chromatography (aluminum oxide, CH_2Cl_2/MeOH 0 up to 2%). The pure compound **15** was isolated by recrystallization from ether (yield: 41%): beige solid; mp 57−59 °C; TLC R_f 0.6 (aluminum oxide, CH_2Cl_2/MeOH 96:4); Anal. ($C_{28}H_{48}ClN_5O_5$, 1.5 H_2O) C, H, N.

***N*¹-((Diethylamino)ethyl)-*N*⁴-((4-methyl-1-oxopentan-2-ylamino)-1-oxopentan-2-yl)terephthalamide (16).** The Weinreb amide **15** (100 mg, 0.19 mmol) reduction was achieved according to method D to afford 50 mg of **16** (yield: 58%). The corresponding hydrochloride was obtained by stirring **16** in ether/HCl 2 N as a very hygroscopic salt: beige solid; mp 72−74 °C; TLC R_f 0.5 (RP-18, solvent mixture B).

***N*¹-((Diethylamino)ethyl)-*N*⁴-(1-(1-(methoxy(methyl)-amino)-4-methyl-1-oxopentan-2-ylamino)-4-methyl-1-oxopentan-2-yl)teraphthalamide (18).** The Weinreb amide **18** was synthesized according to method C with compounds **7** (1.09 g, 4.05 mmol) and **17** (1.89 g, 3.68 mmol) in DMF (30 mL). The crude product (2.13 g) was purified by flash chromatography (aluminum oxide, CH_2Cl_2/gradient of MeOH 0.5 to 2%) to afford 1.78 g of **18** (yield: 75%): white solid; mp 96−98 °C; TLC R_f 0.4 (aluminum oxide, CH_2Cl_2/MeOH 95/5).

***N*¹-((Diethylamino)ethyl)-*N*⁴-(4-methyl-1-(4-methyl-1-(4-methyl-1-oxopentan-2-ylamino)-1-oxopentan-2-ylamino)-1-oxopentan-2-yl)terephthalamide (19).** The reduction of Weinreb amide **18** (0.96 g, 1.5 mmol) was achieved following method D. The pure product was isolated by recrystallization from diethyl ether to afford 0.63 g of **19** (yield: 72%). The hydrochloride salt was precipitated with a solution of ether/HCl 2 N. **19**: white solid; mp 118−120 °C; TLC R_f 0.6 (aluminum oxide, CH_2Cl_2/MeOH 95:5); Anal. ($C_{34}H_{58}ClN_5O_5$, 2.5 H_2O) C, H.

***N*¹-((Diethylamino)ethyl)-*N*⁴-(1-(1-(methoxy(methyl)-amino)-4-methyl-1-oxopentan-2-ylamino)-1-oxo-3-phenylpropan-2-yl)terephthalamide (21).** The synthesis of Weinreb amide **21** was realized according to method C with a solution of compound **7** (0.69 g, 2.53 mmol) and a solution of **20** (1.0 g, 2.3 mmol) in a mixture of CH_2Cl_2 (20 mL)/DMF (10 mL). The crude product was purified by flash chromatography (aluminum oxide, CH_2Cl_2/MeOH 0.5 up to 2%) to afford 0.3 g of **21** (yield: 23%): white solid; mp 101−103 °C; TLC R_f 0.4 (aluminum oxide, CH_2Cl_2/MeOH 95/5); Anal. ($C_{31}H_{45}N_5O_5$, 0.5 H_2O) C, H.

***N*¹-((Diethylamino)ethyl)-*N*⁴-(4-methyl-1-oxo-1-(1-oxo-3-phenylpropan-2-ylamino)pentan-2-yl)terephthalamide (22).** Reduction of Weinreb amide **21** (0.19 g, 0.33 mmol) was achieved according to method D to afford 0.12 g of **22** (71%). The hydrochloride salt was precipitated with a solution of ether/HCl 2 N. **22**: white solid; mp 116−118 °C; TLC R_f 0.5 (aluminum oxide, CH_2Cl_2/MeOH 95:5); Anal. ($C_{29}H_{41}ClN_4O_4$, 4.5 H_2O) C, H, N.

***N*¹-((Diethylamino)ethyl)-*N*⁴-(1-(1-(1-(methoxy(methyl)-amino)-4-methyl-1-oxopentan-2-ylamino)-1-oxo-3-phenylpropan-2-ylamino)-4-methyl-1-oxopentan-2-yl)-terephthalamide (24).** The synthesis of Weinreb amide **24** was realized according to method C with a mixture of compound **7** (1.5 g, 2.53 mmol) and compound **23** (2.65 g, 4.83 mmol) in CH_2Cl_2 (10 mL)/DMF (10 mL). The crude product was purified by flash chromatography (aluminum oxide, CH_2Cl_2/MeOH 0.5 up to 2%) to afford 2.07 g of **24** as a hydrochloride salt (yield: 63%): white solid; mp 92−94 °C; TLC R_f 0.5 (aluminum oxide, CH_2Cl_2/MeOH 95/5); Anal. ($C_{37}H_{56}N_6O_6$, 1.0 H_2O) C, H, N.

***N*¹-((Diethylamino)ethyl)-*N*⁴-(1-(1-(4-methyl-1-oxopentan-2-ylamino)-1-oxo-3-phenylpropan-2-ylamino)-1-oxopentan-2-yl)terephthalamide (25).** The reduction of Weinreb amide **24** (0.45 g, 0.66 mmol) was achieved according to method D to afford 0.26 g of **25** (64%). The hydrochloride salt was precipitated with a solution of ether/HCl 2 N: white solid; mp 127−129 °C; TLC R_f 0.5 (aluminum oxide, CH_2Cl_2/MeOH 95/5); Anal. ($C_{35}H_{52}ClN_5O_5$, 2.5 H_2O) C, H, N.

***N*¹-(2-(Diethylamino)ethyl)-*N*⁴-(1-(1-(1-(methoxy-(methyl)amino)-4-methyl-1-oxopentan-2-ylamino)-4-methyl-1-oxopentan-2-ylamino)-1-oxo-3-phenylpropan-2-yl)-terephthalamide (27).** Weinreb amide **27** was synthesized according to method C from a solution of compound **7** (1.2 g, 4.2 mmol) and a solution of **26** (2.07 g, 3.77 mmol) in a mixture of CH_2Cl_2 (30 mL)/DMF (10 mL). The crude product was purified by flash chromatography (aluminum oxide, CH_2Cl_2/MeOH 0 up to 2%) to afford 1.42 g of **27** (yield: 55%). **27**, HCl: white solid; mp 107−109 °C; TLC R_f 0.5 (aluminum oxide, CH_2Cl_2/MeOH 95/5); Anal. ($C_{37}H_{57}ClN_6O_6$, 2.5 H_2O, 3.5 HCl) C, H, N.

***N*¹-(2-(Diethylamino)ethyl)-*N*⁴-(1-(1-(4-methyl-1-oxopentan-2-ylamino)-4-methyl-1-oxopentan-2-ylamino)-1-oxo-3-phenylpropan-2-yl)terephthalamide (28).** The reduction of Weinreb amide **27** (1.80 g, 2.64 mmol) was achieved according to method D to afford 0.72 g of **28** (41%). The hydrochloride salt was precipitated with a solution of ether/HCl 2 N. **28**: white solid; mp 128−130 °C; TLC R_f 0.6 (RP-18, solvent mixture B); Anal. ($C_{35}H_{52}ClN_5O_5$, 3.5 H_2O) C, H, N.

Cytotoxicity Assay. Attached human ocular melanoma IPC227F cells were seeded in 96 well plates and incubated for 24 h at 37 °C in a humidified atmosphere under 5% CO_2 with a standard medium (DMEM and 10% calf fetal serum). After the addition of fresh medium containing increasing concentrations of drugs previously prepared in DMSO (final concentration 0.025%), cells were incubated for 48 h for the determination of IC_{50}, washed with 1X PBS buffer, and then frozen at −80 °C. After thawing at room temperature, cells were incubated for 1 h at room temperature with a 0.01% SDS solution, frozen again at −80 °C, and then thawed again at room temperature. The Hoechst dye 33342 solution was added to each sample (final concentration 15 μg/mL), and plates were incubated for 1 h at room temperature on a plate shaker in the dark. Fluorescence was measured using a fluorescence microplate reader at 360/460 nm (Fluoroskan Ascent FL; Labsystems, Farnborough, Hampshire), and cell survival rates (percent cell survival relative to untreated control) were calculated. The cytotoxic activity of drugs was expressed as the concentration inhibiting cell growth by 50% (IC_{50}) calculated from the survival curves.

Western Blot. IPC227F cells cultured in 10 cm diameter dishes were treated with 10 μM cytotoxic drugs prepared in DMSO and diluted in fresh culture medium (final concentration of DMSO 0.025%) for various incubation times. Control cells were cultured with a standard medium and DMSO 0.025%. Cells were then scraped off and centrifuged for 8 min at 440*g* and 4 °C. The cell pellets were lysed with 100 μL of lysis buffer (50 mM Tris (pH = 7.5), 120 mM NaCl, 0.5% NP40, and 1X protease inhibitors) for 15 min on ice and sonicated for three pulses of 15 s, at 50% output power, using a Microsom XL ultrasonic cell disrupter from Heat Systems. Lysates were then centrifuged for 10 min at 10000*g* and 4 °C to remove cellular debris, and the supernatant protein concentration was determined according to Bradford[62] with bovine serum albumin as the standard. Equal amounts of total cell lysates (100 μg) were resolved on 7.5% SDS−PAGE and transferred onto nitrocellulose membranes. The membranes were incubated for 2 h in a blocking solution (25 mM Tris (pH = 8), 125 mM NaCl, 0.1% Tween-20, 4% nonfat dried milk) and then reacted overnight at room temperature with a primary monoclonal antibody raised against ubiquitin at a 1/1000 dilution (FK2; Affiniti Research Products Limited, U.K.). Membranes were then incubated for 1 h with a mouse peroxidase-conjugated secondary antibody (1/5000). Ubiquitin-tagged proteins were detected by the enhanced chemiluminescence (ECL) detection system (Amersham Biosciences, Burckinghamshire, England).

20S Proteasome Inhibition Assays. The chymotrypsin-like, trypsin-like, and peptidyl glutamyl peptide hydrolase activities of 20S proteasomes were measured as follows. 0.5−1 μg of 20S mammalian proteasomes (Affiniti) were incubated for 30 min at room temperature in the presence of 0.1, 1, and

10 μM **19**, **25**, and **28**, and MG132 or epoxomicin (Affiniti) as controls, in a 50 mM Tris-HCl (pH = 8) buffer. 100 μM fluorogenic proteasomes substrates Suc-LLVY-AMC (Affiniti) and Boc-LRR-AMC (Affiniti) or 200 μM Z-LLE-AMC (Calbiochem) in DMSO were then added to assay solutions, and samples were incubated for 1 h at 37 °C in a 96 well black microtiter plate. The final reaction volume was 100 μL. The final DMSO concentration was 1%. The reaction was stopped by adding 100 μL of 10% SDS, and fluorescence was determined by measuring the release of AMC using a fluorescence microplate reader at 360/460 nm.

Flow Cytometric Analysis. M4Beu cells (human melanoma cells) or normal melanocytes (MshL1) were incubated with 10 mM compound **19** or MG132 for 24 h. The flow cytometric analysis of cell DNA content was performed using an Epics XL (Coulter, Hialeah, FL) after propidium iodide labeling of cells. Fluorescence attributable to PI was determined using excitation by an argon laser, operating at 488 nm and a power output of 15 mW. For each histogram, the cell distribution was calculated using the Multicycle software program (Phoenix, Flow Systems, San Diego, CA) and expressed by the ratio of compound **19**/control or MG132/control in normal melanocytes or M4Beu cells.

Acknowledgment. We thank Dr. M. Borel for the proton and carbon magnetic resonance spectra performed on the Bruker DRX 500. We also thank M. Bayle for the synthesis of several intermediates. We are grateful for many helpful discussions throughout the course of this work with Dr. J. Helfenbein and Dr. M.-F. Moreau.

Supporting Information Available: Main fragmentations of $[M + H]^+$ ions derived from electrospray of Weinreb amides **12**, **15**, **18**, **21**, **24**, and **27** and spectroscopic data. This information is available free of charge via the Internet at http://pubs.acs.org.

References

(1) Coux, O.; Tanaka, K.; Goldberg, A. L. Structure and Functions of the 20S and 26S Proteasomes. *Annu. Rev. Biochem.* **1996**, *65*, 801−847.
(2) Goldberg, A. L.; Rock, K. L. Proteolysis, Proteasomes and Antigen Presentation. *Nature* **1992**, *357*, 375−378.
(3) Groettrup, G.; Schmidtke, G. Selective Proteasome Inhibitors: Modulators of Antigen Presentation? *DDT* **1999**, *4* (2), 63−71.
(4) Elliott, P. J.; Zollner T. M.; Boehncke, W.-H. Proteasome Inhibition: a New Anti-inflammatory Strategy. *J. Mol. Med.* **2003**, *81*, 235−245.
(5) Price, S. R. Increased Transcription of Ubiquitin-proteasome System Components: Molecular Responses Associated with Muscle Atrophy. *Int. J. Biochem. Cell Biol.* **2003**, *35*, 617−628.
(6) Goellner, G. M.; Rechsteiner, M. Are Hungtington's and Polyglutamine-based Ataxias Proteasome Storage Diseases? *Int. J. Biochem. Cell Biol.* **2003**, *35*, 562−571.
(7) Naidoo, N.; Song, W.; Hunter-Ensor, M.; Sehgal, A. A Role for the Proteasome in the Light Response of the Timeless Clock Protein. *Science* **1999**, *285*, 1737−1741.
(8) Hilt, W.; Wolf, D. H. Proteasomes: Destruction as a Programme. *Trends Biochem. Sci*. **1996**, *21*, 96−102.
(9) Myung, J.; Kim, K. B.; Crews, C. M. The Ubiquitin-Proteasome Pathway and Proteasome Inhibitors. *Med. Res. Rev*. **2001**, *21* (4), 245−273.
(10) Adams, J.; Palombella, V. J.; Sausville, E. A.; Johson, J.; Destree, A.; Lazarus, D. D.; Maas, J.; Pien, C. S.; Prakash, S.; Elliott, P. J. Proteasome Inhibitors: a Novel Class of Potent and Effective Antitumor Agents. *Cancer Res.* **1999**, *59*, 2615−2622.
(11) Kisselev, A. F.; Goldberg, A. L. Proteasome Inhibitors: from Research Tools to Drug Candidates. *Chem. Biol.* **2001**, *8*, 739−758.
(12) Gillessen, S.; Groettrup, M.; Cerny, T. The proteasome, a New Target for Cancer Therapy. *Onkologie* **2002**, *25*, 534−539.
(13) Adams, J. Potential for Proteasome Inhibition in the Treatment of Cancer. *Drug Discovery Today* **2003**, *8* (7), 307−315.
(14) Los, M.; Burek, C. J.; Stroh, C.; Benediyk, K., Hug, H.; Mackiewicz, A. Anticancer Drugs of Tomorrow: Apoptotic Pathways as Targets for Drug Design. *Drug Discovery Today* **2003**, *8* (2), 67−77.
(15) Masse, C. E.; Morgan, A. J., Adams, J.; Panek, J. S. Syntheses and Biological Evaluation of (+)-Lactacystin and Analogues. *Eur. J. Org. Chem.* **2000**, 2513−2528.
(16) Dick, L. R.; Cruikshank, A. A.; Destree, A. D.; Grenier, L.; McCormack, T. A.; Melandri, F. D.; Nunes, S. L.; Palombella, V. J.; Parent, L. A.; Plamondon, L.; Stein, R. L. Mechanistic Studies on the Inactivation of the Proteasome by Lactacystin in Cultured Cells. *J. Biol. Chem.* **1997**, *272*, 182−188.
(17) Fenteany, G.; Schreiber, S. L. Lactacystin, Proteasome Function, and Cell Fate. *J. Biol. Chem.* **1998**, *273* (15), 8545−8548.
(18) Kohno, J.; Koguchi, Y.; Nishio, M.; Nakao, K.; Kuroda, M.; Shimizu, R.; Ohnuki, T.; Komatsubara, S. Structures of TMC-95A−D: Novel Proteasome Inhibitors from *Apiospora montagnei* Sacc. TC 1093. *J. Org. Chem*. **2000**, *65*, 990−995.
(19) Vinitsky, A.; Michaud, C.; Powers, J. C.; Orlowski, M. Inhibition of the Chymotrypsin-like Activity of the Pituitary Multicatalytic Proteinase Complex. *Biochemistry* **1992**, *31*, 9421−9428.
(20) Wilk, S.; Figueiredo-Preira, M. E. Synthetic Inhibitors of the Multicatalytic Proteinase Complex (Proteasome). *Enzyme Proteine* **1993**, *47*, 306−313.
(21) Vinitsky, A.; Cardozo, C.; Sepp-Lorenzino, L.; Michaud, C.; Orlowski, M. Inhibition of the Proteolytic Activity of the Multicatalytic Proteinase Complex (Proteasome) by Substrate-related Peptidyl Aldehydes. *J. Biol. Chem.* **1994**, *269*, 29860−29866.
(22) Cardozo, C.; Vinitsky, A.; Michaud, C.; Orlowski, M. Evidence That the Nature of Amino Acid Residues in the P3 Position Directs Substrates to Distinct Catalytic Sites of the Pituitary Multicatalytic Proteinase Complex (Proteasome). *Biochemistry* **1994**, *33* (21), 6483−6489.
(23) Adams, J.; Behnke, M.; Chen, S.; Cruickshank, A. A.; Dick, L. R.; Grenier, L.; Klunder, J. M.; Ma, Y.-T.; Plamondon, L.; Stein, R. L. Potent and Selective Inhibitors of the Proteasome: Dipeptidyl Boronic Acids. *Bioorg. Med. Chem. Lett*. **1998**, *8*, 333−338
(24) Lightcap, E. S.; McCormack, T. A.; Pien, C. S.; Chau, V.; Adams, J.; Elliott, P. J. Proteasome Inhibition Measurements: Clinical Application. *Clin. Chem.* **2000**, *46* (5), 673−683.
(25) Bogyo, M.; McMaster, J. S.; Gaczynska, M.; Tortorella, D.; Goldberg, A. L.; Ploegh, H. Covalent Modification of the Active Site Threonine of Proteosomal β-subunits and the *Escherichia coli* Homologue HsIV by a New Class of Inhibitors. *Proc. Natl. Acad. Sci. U.S.A.* **1997**, *94* (13), 6629−6634.
(26) Bogyo, M.; Shin, S.; McMaster, J. S.; Ploegh, H. L. Substrate Binding and Sequence Preference of the Proteasome Revealed by Active-site-directed Affinity Probes. *Chem. Biol.* **1998**, *5* (6), 307−320.
(27) Elofsson, M.; Splittgerber, U.; Myung, J.; Mohan, R.; Crews, C. M. Towards Subunit-Specific Proteasome Inhibitors: Synthesis and Evaluation of Peptide α',β'-epoxycetones. *Chem. Biol*. **1999**, *6* (11), 811−822.
(28) Lynas, J. F.; Harriott, P.; Healy, A.; McKervey, M. A.; Walker, B. Inhibitors of the Chymotrypsin-like Activity of Proteasome Based on di- and tri-peptidyl α-keto aldehydes (glyoxals). *Bioorg. Med. Chem. Lett.* **1998**, *8*, 373−378.
(29) Lum, R. T.; Nelson, M. G.; Joly, A.; Horsma, A. G.; Lee, G.; Meyer, S. M.; Wick, M. M.; Schow, S. R. Selective Inhibition of the Chymotrypsin-like Activity of the 20S Proteasome by 5-methoxy-1-indanone Dipeptide Benzamides. *Bioorg. Med. Chem. Lett.* **1998**, *8*, 209−214.
(30) Loidl, G.; Groll, M.; Musiol, H. J.; Huber, R.; Moroder, L. Bivalency as a Principle for Proteasome Inhibition. *Proc. Natl. Acad. Sci. U.S.A.* **1999**, *96*, 5418−5422.
(31) Loidl, G.; Groll, M.; Musiol, H.-J.; Ditzel, L.; Huber, R.; Moroder, L. Bifunctional Inhibitors of the Trypsin-like Activity of Eukaryotic Proteasomes. *Chem. Biol.* **1999**, *6* (4), 197−204.
(32) Löwe, J.; Stock, D.; Jap, B.; Zwickl, P.; Baumeister, W.; Hubert, R. Crystal Structure of the 20S Proteasome from the Archaeon T. acidophilum at 3.4 Å Resolution. *Science* **1995**, *268* (5210), 533−539.
(33) Groll, M.; Ditzel, L.; Löwe, J.; Stock, D.; Bochtler, M.; Bartunik, H. D.; Huber, R. Structure of 20S Proteasome from Yeast at 2.4 Å Resolution. *Nature* **1997**, *386* (6624), 463−471.
(34) Goldberg, A. L.; Akopian, T. N.; Kisselev, A. F.; Lee, A. H.; Rohrwild, M. New Insights into the Mechanisms and Importance of the Proteasome in Intracellular Protein Degradation. *Biol. Chem*. **1997**, *378*, 131−140.
(35) Ditzel, L.; Stock, D.; Löwe, J. Structural Investigation of Proteasome Inhibition. *Biol. Chem.* **1997**, *378*, 239−247.
(36) Groll, M.; Heinemeyer, W.; Jäger, S.; Ullrich, T.; Bochtler, M.; Wolf, D. H.; Huber, R. The Catalytic Sites of 20S Proteasomes and their Role in Subunit Maturation: A Mutational and Crystallographic Study. *Proc. Natl. Acad. Sci. U.S.A.* **1999**, *96*, 10976−10983.
(37) Teicher, B. A.; Ara, G.; Herbst, R.; Palombella, V. J.; Adams, J. The Proteasome Inhibitor PS-341 in Cancer Therapy. *Clin. Cancer Res.* **1999**, *5*, 2638−2645.
(38) Adams, J. Development of the Proteasome Inhibitor PS-341. *Oncologist* **2002**, *7*, 9−16.
(39) Stein, R. L.; Ma, Y.-T.; Brand, S. Inhibitors of The 26S Proteolytic Complex And The 20S Proteasome Contained Therein. U.S. Patent 5,693,617, December 2, 1997.

(40) Moreau, M. F.; Michelot, J.; Veyre, A.; Madelmont, J. C.; Godenèche, D.; Labarre, P.; Parry, D.; Meyniel, G. Agents pour le Diagnostic et le Traitement des Mélanomes, Dérivés Halogénés Aromatiques Utilisables comme de tels Agents et leur Préparation. French patent 8901898, February 14, 1989.
(41) Michelot, J. M.; Moreau, M. F. C.; Labarre, P. G.; Madelmont, J. C.; Veyre, A. J.; Papon, J. M.; Parry, D. F.; Bonafous, J. F.; Boire, J. Y. P.; Desplanches, G. G.; Bertrand, S. J.; Meyniel, G. Synthesis and Evaluation of New Iodine-^{125} radiopharmaceutical as Potential Tracers for Malignant Melanoma. *J. Nucl. Med.* **1991**, *32*, 1573−1580.
(42) Moreau, M. F.; Madelmont, J. C.; Michelot, J.; Labarre, P.; Veyre, A.; Papon, J.; Batle, M.; Boire, J. Y.; Desplanches, G.; Meyniel, G. New ^{125}I-radiopharmaceuticals for Diagnosis and Treatment for Malignant Melanoma. *Eur. J. Nucl. Med.* **1993**, *18*, 538.
(43) Michelot, J.; Veyre, A.; Bonafous, J.; Moreau, M. F.; Madelmont, J. C.; Papon, J.; Labarre, P.; Bacin, F.; Kauffman, P.; Plagne, R. Imaging of Malignant Melanoma and Metastases with ^{123}I−BZA. *Melanoma Res.* **1993**, *3*, 83.
(44) Michelot, J. M.; Moreau, M. F. C.; Veyre, A. J.; Bonafous, J. F.; Bacin, F. J.; Madelmont, J. C.; Bussiere, F.; Souteyrand, P. A.; Mauclaire, L. P.; Chossat, F. M.; Papon, J. M.; Labarre, P. G.; Kauffman, Ph.; Plagne, R. J. Phase II Scintigraphic Clinic Trial of Malignant Melanoma and Metastases with Iodine-^{123}-N−(2-diethylaminoethyl-4-iodobenzamide). *J. Nucl. Med.* **1993**, *34*, 1260−1266.
(45) Moreau, M. F.; Michelot, J.; Papon, J.; Bayle, M.; Labarre, P.; Madelmont, J. C.; Parry, D.; Boire, J. Y.; Segquin, H.; Veyre, A.; Mauclaire, L. Synthesis, Radiolabeling, and Preliminary Evaluation in Mice of some (N-diethylaminoethyl)-4-iodobenzamide Derivates as Melanoma Imaging Agents. *Nucl. Med. Biol.* **1995**, *22*, 737−747.
(46) Chehade, F.; Michelot, J.; Hindie, E.; Papon, J.; Delabriolle-Vaylet, C.; Zhang, L.; Escaig, F.; Moreau, M. F.; Veyre, A. Localization of N−(2-diethylaminoethyl)-4-iodobenzamide in the Pigmented Mouse Eye: a Microanalytical Study. *Cell. Mol. Biol.* **1996**, *42*, 343−350.
(47) Moins, N.; D'Incan, M.; Bonafous, J.; Bacin, F.; Labarre, P.; Moreau, M. F.; Mestas, D.; Noirault, E.; Chossat, F.; Berthommier, E.; Papon, J.; Bayle, M.; Souteyrand, P.; Madelmont, J. C.; Veyre, A. ^{123}I-*N*-(2-diethyleminoethyl)-2-iodobenzamide: a potential imaging agent for cutaneous melanoma staging. *Eur. J. Nucl. Med.* **2002**, *29*, 1478−1484.
(48) Maul, W. Synthese von 14C-markiertem Noxiptilin. *J. Labelled Compd.* **1969**, *3*, 251−256.
(49) Gilman, H. Some Personnal Notes on More Than One-Half Century of Organometallic Chemistry. *Organomet. Chem.* **1968**, *7*, 1−52.
(50) Corey, E. J.; Székely, I.; Shiner, C. S. *Tetrahedron Lett.* **1977**, 3529.
(51) Klausner, Y. S.; Bodansky, M. Coupling Reagents in Peptide Synthesis. *Synthesis* **1972**, 453−463.
(52) Sheeman, J.C.; Goodman, M.; Hess, G. P. Peptide Derivatives Containing Hydroxyamino Acids. *J. Am. Chem. Soc*. **1956**, *78*, 1367−1369.
(53) Sheeman, J. C.; Hess, G. P. A New Method of Forming Peptide Bonds. *J. Am. Chem. Soc.* **1955**, *77*, 1067−1068.
(54) Smith, M.; Moffatt, J. G.; Khorana, H. G. Carbodiimides. VIII.[1] Observations on the Reactions of Carbodiimides with Acids and Some New Applications in the Synthesis of Phosphoric Acid Esters. *J. Am. Chem. Soc.* **1958**, *80*, 6204−6212.
(55) Khorana, H. G. The Chemistry of Carbodiimides. *Chem. Rev.* **1953**, *53*, 145−166.
(56) DeTar, D. F.; Silverstein, R. Reactions of Carbodiimides. I. The Mechanisms of the Reactions of Acetic Acid with Dicyclohexylcarbodiimide.[1,2] *J. Am. Chem. Soc.* **1966**, *88*, 1013−1019.
(57) DeTar, D. F.; Silverstein, R. Reactions of Carbodiimides. II. The Reactions of Dicyclohexylcarbodiimide with Carboxylic Acids in the Presence of Amines and Phenols.[1,2] *J. Am. Chem. Soc.* **1966**, *88*, 1020−1023.
(58) DeTar, D. F.; Silverstein, R.; Rogers, F. F., Jr.; Reactions of carbodiimides. III. The reactions of carbodiimides with Peptide Acids.[1,2] *J. Am. Chem. Soc.* **1966**, *88*, 1024−1030.
(59) Lebreton, L.; Annat, J.; Derrepas, P.; Dutartre, P.; Renaut, P. Structure-Immunosuppressive Activity Relationships of New Analogues of 15-Deoxyspergualin.1. Structural Modifications of the Hydroglycine Moiety. *J. Med. Chem.* **1999**, *42*, 277−290.
(60) Hochstrasser, M. Ubiquitin, Proteasomes, and the Regulation of Intracellular Protein Degradation. *Curr. Opin. Cell Biol.* **1995**, *7*, 215−223.
(61) Viestra, R. D. The Ubiquitin/26S Proteasome Pathway, the Complex Last Chapter in the Life of Many Plant Proteins. *Trends Plant Sci.* **2003**, *8* (3), 135−142.
(62) Bradford, M. M. A rapid and sensitive method for the quantitation of microgram quantitities of protein utilizing the principle of protein-dye binding. *Anal. Biochem.* **1976**, *72*, 248.

JM050181L